Cramer-Rao bounds for acoustic emission events localization in a flat plate

A. Le Duff, S.E. Hamdi, G. Plantier, A. Sourice and R. Feron

Groupe ESEO, rue Merlet de la Boulaye, 49009 Angers, France
alain.le_duff@eseo.fr

This article addresses the problem of 2D location of acoustics source in a plate. This location is based on Time Difference of Arrival (TDOA) measurements thanks to an array of three sensors arbitrary distributed on the 2D plane. In order to obtain a fast, but robust and accuracy, algorithm, allowing an online estimation of the location of hits or Acoustic Emission events in a composite plate for example, the authors propose an exact solution of the TDOA problem by solving a nonlinear system of coupled equations. The exact analytical Cramer-Rao Bounds (CRBs) on the variance of the estimations is then presented. Moreover, the statistical performances of the method are illustrated by means of Monte-Carlo simulations and are compared to the CRBs.

1 Introduction

The monitoring of Acoustic Emission events in composite material needs not only the identification of the nature and the instant of occurrence of the events but the location of the acoustic source. A previous work proposed a method, based on a short-time crosscorrelation function, which can be used for online Acoustic Emission source location in a composite plate [1]. This method allows to estimate the time delay in the early coherent part of the signals, which is especially suitable in a very dispersive medium such as composite material. These estimated time delay can be used with 3 distributed sensors in a two-dimensional plate for sound source location. Some previous works proposed approximated solutions or maximum likelihood methods [2, 3, 4]. In this paper, the authors present the exact solution of the Time Difference Of Arrival (TDOA) problem which can be used for Acoustic Emission source location in a simple way. Moreover, in order to estimate the a priori accuracy of the technic and the effect of the individual arrival times errors, the exact Cramer-Rao Bound for the estimated source position, are proposed. These last expressions can be very useful in order to justify the accuracy of TDOA measurements and for guiding the choice of the sensors position.

2 Theoretical analysis

2.1 Location calculation

The basic principle for the location calculation is the time-distance relationship implied by the velocity of the acoustic wave. The arrival time t on an acoustic event combine with the sound velocity c, leads to the distance d from the acoustic source to the sensor:

$$d = c \cdot t. \tag{1}$$

Then, each arrival time difference between two sensors implies a difference in distance and leads to the distance equation

$$d_{kl} = \sqrt{(x-x_k)^2 + (y-y_k)^2} - \sqrt{(x-x_l)^2 + (y-y_l)^2}, \tag{2}$$

where (x, y), (x_k, y_k), and (x_l, y_l) are the unknown coordinates of the source and the coordinates, supposed to be known, of the sensors k and l respectively ($k = 1, 2, 3$, $l = 1, 2, 3$).

By considering sensor 1 as the reference sensor, it may be possible to consider two distance equations. The solution, which corresponds to the intersection of two hyperbolas as shown in Fig. 1(a), can be solved and leads to the next algorithm:

1. Recording of the 3 sensors location, $x_1, y_1, x_2, y_2, x_3, y_3$;
2. Distance calculation from time delay measurements:
$$d_{21} = c \cdot t_{21} \tag{3}$$
and
$$d_{31} = c \cdot t_{31} \tag{4}$$
where $t_{21} = t_2 - t_1$ and $t_{31} = t_3 - t_1$ are the arrival time difference between sensors 2 and 1 and sensors 3 and 1 respectively;
3. Calculation of the coefficients
$$\alpha_{21} = \frac{-d_{21}^2 - x_1^2 + x_2^2 - y_1^2 + y_2^2}{2} \tag{5}$$
and
$$\alpha_{31} = \frac{-d_{31}^2 - x_1^2 + x_3^2 - y_1^2 + y_3^2}{2}; \tag{6}$$
4. Calculation of the parameters
$$a = -\frac{(x_1 - x_2)d_{31} - (x_1 - x_3)d_{21}}{(y_1 - y_2)d_{31} - (y_1 - y_3)d_{21}} \tag{7}$$
and
$$b = -\frac{\alpha_{21}d_{31} - \alpha_{31}d_{21}}{(y_1 - y_2)d_{31} - (y_1 - y_3)d_{21}}; \tag{8}$$
5. Calculation of the coefficients
$$A = [(x_1 - x_2) + a(y_1 - y_2)]^2 - d_{21}^2(1 + a^2), \tag{9}$$
$$B = 2\{[\alpha_{21} + b(y_1 - y_2)][(x_1 - x_2) + a(y_1 - y_2)] - d_{21}^2[a(b - y_1) - x_1]\}, \tag{10}$$
and
$$C = [\alpha_{21} + b(y_1 - y_2)]^2 - d_{21}^2[x_1^2 + (b - y_1)^2]; \tag{11}$$
6. Calculation of the coordinates:
$$x = \frac{-B \pm \sqrt{B^2 - 4AC}}{2A} \tag{12}$$
and
$$y = ax + b. \tag{13}$$

2.2 Cramer-Rao Bounds

In this work, the authors propose the exact analytic forms of the CRBs. These bounds, expressed as functions of the sensors location and the variance σ^2 of the time delay estimation τ, indicate the lower limits of the estimation variance for the unknown coordinates x and y of the acoustic source.

2.2.1 Probality density function of the measurement signal

Let the observed data be

$$\tau_{21} = t_{21} + b_{21} \tag{14}$$

and

$$\tau_{31} = t_{31} + b_{31} \tag{15}$$

where the observation noises, b_{21} and b_{31} are white additive Gaussian processes. Then, the probability density functions of the observations are given by

$$p(\tau_{m1};\theta) = \frac{1}{\sqrt{2\pi\sigma^2}} \exp\left[-\frac{1}{2\sigma^2}(\tau_{m1} - t_{m1})^2\right] \tag{16}$$

with $m = 1, 2$ and $\theta = [x, y]^T$ the unknown coordinates of the source. Since τ_{21} and τ_{31} are non-correlated, then

$$\begin{aligned} p(\tau;\theta) &= p(\tau_{21};\theta) \times p(\tau_{31};\theta) \\ &= \frac{1}{\sqrt{2\pi\sigma^2}} \exp\left\{-\frac{\left[(\tau_{21} - t_{21})^2 + (\tau_{31} - t_{31})^2\right]}{2\sigma^2}\right\} \end{aligned} \tag{17}$$

with $\tau = [\tau_{21}, \tau_{31}]^T$.

The log-likelihood function is then given by

$$\begin{aligned} \wedge(\tau;\theta) &= \ln\left[p(\tau;\theta)\right] \\ &= -N\ln(2\pi\sigma^2) - \frac{\left[(\tau_{21} - t_{21})^2 + (\tau_{31} - t_{31})^2\right]}{2\sigma^2} \end{aligned} \tag{18}$$

2.2.2 Fisher Information Matrix

The CRB is the inverse of the Fisher Information Matrice (FIM) [5] whose elements are

$$[\mathbf{I}(\theta)]_{ij} = -E\left[\frac{\partial^2 \wedge(\tau;\theta)}{\partial\theta_i\partial\theta_j}\right] \tag{19}$$

with $i = 1, 2$ and $j = 1, 2$. Thus, in order to evaluate the FIM, derivatives of $\wedge(\tau;\theta)$ need to be computed. It can be shown that the derivative of $\wedge(\tau;\theta)$ with respect to θ_i is given by

$$\frac{\partial \wedge(\tau;\theta)}{\partial\theta_i} = -\frac{1}{2\sigma^2}\frac{\partial}{\partial\theta_i}\left[(\tau_{21} - t_{21})^2 + (\tau_{31} - t_{31})^2\right] \tag{20}$$

However

$$\frac{\partial}{\partial\theta_i}\left[(\tau_{21} - t_{21})^2\right] = -2(\tau_{21} - t_{21})\frac{\partial t_{21}}{\partial\theta_i} \tag{21}$$

and

$$\frac{\partial}{\partial\theta_i}\left[(\tau_{31} - t_{31})^2\right] = -2(\tau_{31} - t_{31})\frac{\partial t_{31}}{\partial\theta_i}. \tag{22}$$

Moreover

$$t_{21} = \frac{d_{21}}{c} = \frac{l_2 - l_1}{c} \tag{23}$$

and

$$t_{31} = \frac{d_{31}}{c} = \frac{l_3 - l_1}{c} \tag{24}$$

with

$$l_1 = \sqrt{(x - x_1)^2 + (y - y_1)^2} \tag{25}$$

$$l_2 = \sqrt{(x - x_2)^2 + (y - y_2)^2} \tag{26}$$

and

$$l_3 = \sqrt{(x - x_3)^2 + (y - y_3)^2}. \tag{27}$$

Then

$$\frac{\partial t_{m1}}{\partial\theta_i} = \frac{1}{c}\left(\frac{\partial l_m}{\partial\theta_i} - \frac{\partial l_1}{\partial\theta_i}\right) \tag{28}$$

with

$$\frac{\partial l_m}{\partial\theta_i} = \frac{\theta_i - \theta_{i_m}}{l_m}. \tag{29}$$

and

$$m = 2, 3.$$

Hence

$$\begin{aligned} \frac{\partial \wedge(\tau;\theta)}{\partial\theta_i} &= \frac{1}{c\sigma^2}(\tau_{21} - t_{21})\left(\frac{\theta_i - \theta_{i2}}{l_2} - \frac{\theta_i - \theta_{i1}}{l_1}\right) \\ &+ \frac{1}{c\sigma^2}(\tau_{31} - t_{31})\left(\frac{\theta_i - \theta_{i3}}{l_3} - \frac{\theta_i - \theta_{i1}}{l_1}\right) \end{aligned} \tag{30}$$

The second order derivatives of $\wedge(\tau;\theta)$ are then given by

$$\begin{aligned} &\frac{\partial}{\partial\theta_j}\left[\frac{\partial \wedge(\tau;\theta)}{\partial\theta_i}\right] \\ &= \frac{1}{c\sigma^2}\left\{-\frac{1}{c}\left(\frac{\theta_j - \theta_{j_2}}{l_2} - \frac{\theta_j - \theta_{j_1}}{l_1}\right)\left(\frac{\theta_i - \theta_{i_2}}{l_2} - \frac{\theta_i - \theta_{i_1}}{l_1}\right)\right. \\ &- \frac{1}{c}\left(\frac{\theta_j - \theta_{j_3}}{l_3} - \frac{\theta_j - \theta_{j_1}}{l_1}\right)\left(\frac{\theta_i - \theta_{i_3}}{l_3} - \frac{\theta_i - \theta_{i_1}}{l_1}\right) \\ &+ (\tau_{21} - \tau_{21})\left[\frac{(\theta_i - \theta_{i_2})(\theta_j - \theta_{j_2})}{l_2^3} - \frac{(\theta_i - \theta_{i_1})(\theta_j - \theta_{j_1})}{l_1^3}\right] \\ &+ \left.(\tau_{31} - \tau_{31})\left[\frac{(\theta_i - \theta_{i_3})(\theta_j - \theta_{j_3})}{l_3^3} - \frac{(\theta_i - \theta_{i_1})(\theta_j - \theta_{j_1})}{l_1^3}\right]\right\} \end{aligned} \tag{31}$$

with $i \neq j$. When $i = j$

$$\begin{aligned} &\frac{\partial}{\partial\theta_j}\left[\frac{\partial \wedge(\tau;\theta)}{\partial\theta_i}\right] \\ &= \frac{1}{c\sigma^2}\left\{-\frac{1}{c}\left(\frac{\theta_j - \theta_{j_2}}{l_2} - \frac{\theta_j - \theta_{j_1}}{l_1}\right)^2\right. \\ &\quad -\frac{1}{c}\left(\frac{\theta_j - \theta_{j_3}}{l_3} - \frac{\theta_j - \theta_{j_1}}{l_1}\right)^2 \\ &+ (\tau_{21} - \tau_{21})\left[\frac{(\theta_i - \theta_{i_2})^2}{l_2^3} - \frac{(\theta_i - \theta_{i_1})^2}{l_1^3} + \frac{1}{l_2} - \frac{1}{l_1}\right] \\ &+ \left.(\tau_{31} - \tau_{31})\left[\frac{(\theta_i - \theta_{i_3})^2}{l_3^3} - \frac{(\theta_i - \theta_{i_1})^2}{l_1^3} + \frac{1}{l_3} - \frac{1}{l_1}\right]\right\} \end{aligned} \tag{32}$$

By noting that

$$K_{j2} = \left(\frac{\theta_j - \theta_{j_2}}{l_2} - \frac{\theta_j - \theta_{j_1}}{l_1}\right) \tag{33}$$

and

$$K_{j3} = \left(\frac{\theta_j - \theta_{j_3}}{l_3} - \frac{\theta_j - \theta_{j_1}}{l_1}\right) \tag{34}$$

it can be shown that the expected values are

$$-E\left[\frac{\partial^2 \wedge(\tau;\theta)}{\partial\theta_i\partial\theta_j}\right] = \frac{1}{c^2\sigma^2}\left(K_{j2}\cdot K_{i2} + K_{j3}\cdot K_{i3}\right) \quad (i \neq j) \tag{35}$$

and

$$-E\left[\frac{\partial^2 \wedge(\tau;\theta)}{\partial\theta_i^2}\right] = \frac{1}{c^2\sigma^2}\left(K_{i2}^2 + K_{i3}^2\right) \quad (i = j). \tag{36}$$

The FIM is then given by

$$\mathbf{I}(\theta) = \frac{1}{c^2\sigma^2}\begin{bmatrix} K_{12}^2 + K_{13}^2 & K_{22}\cdot K_{12} + K_{23}\cdot K_{13} \\ K_{12}\cdot K_{22} + K_{13}\cdot K_{23} & K_{22}^2 + K_{23}^2 \end{bmatrix} \tag{37}$$

2.2.3 Cramer Rao Bound

Inverting this matrix gives the CRB for the parameters. Then, the CRB for $\theta_1 = x$ and $\theta_2 = y$ are

$$\mathrm{CRB}(\theta_1) = \mathrm{CRB}(x) = c^2\sigma^2 \times \frac{K_{22}^2 + K_{23}^2}{(K_{12}K_{23} - K_{13}K_{22})^2}, \tag{38}$$

and

$$\mathrm{CRB}(\theta_2) = \mathrm{CRB}(y) = c^2\sigma^2 \times \frac{K_{12}^2 + K_{13}^2}{(K_{12}K_{23} - K_{13}K_{22})^2} \tag{39}$$

with

$$K_{12} = \frac{x - x_2}{l_2} - \frac{x - x_1}{l_1}, \tag{40}$$

$$K_{13} = \frac{x - x_3}{l_3} - \frac{x - x_1}{l_1}, \tag{41}$$

$$K_{22} = \frac{y - y_2}{l_2} - \frac{y - y_1}{l_1}, \tag{42}$$

and

$$K_{23} = \frac{y - y_3}{l_3} - \frac{y - y_1}{l_1}. \tag{43}$$

In these expressions,

$$l_k = \sqrt{(x - x_k)^2 + (y - y_k)^2} \quad (k = 1, 2, 3) \tag{44}$$

represents the Euclidean distance between the source location and sensor k.

3 Results and conclusions

At last, the statistical behavior of the location procedure is performed. Arbitrary units (a.u.) has been chosen to describe each physical quantities. The parameters of the problem are $c = 1$, $(x_1, y_1) = (5, 8.5)$ (reference sensor), $(x_2, y_2) = (1, 1.5)$ and $(x_3, y_3) = (9, 1.5)$. 1000 Monte Carlo trials were run on simulated data and for an arbitrary position of the three sensors as described by figure 1(a). The black area, shown in figure 1(b), indicates the valid zone of measurement, *i.e.* the area where no error was encountered during the simulation (the hyperbolas always intersect each other).

Then, the performances of the localization procedure is compared the theorical CRB (Équations 38 and 39). Figure 2 shows that the variance of the position estimation, obtained with a noise variance of the time delay given by $\mathrm{var}(\tau) = 0.05$, is very close to the CRB in the valid area. In order to assess the performance of the estimator for different error level, 1000 source localization estimations, using different noise realizations lying between 0.001 and 8.192, has been performed for a same coordinate pair $(x, y) = (4.5, 4.5)$. The results (figure 3) show that the performance of the algorithm still follows the theorical variance when the time error is low enough ($\mathrm{var}(\tau) \leqslant 1$). This study provides a simple way to determine the optimal position of a sensor array for a given a-priori accuracy. Now, an experimental set-up is going to be developed for an experimental assessment of the method.

References

[1] A. Le Duff, S.E. Hamdi, G. Plantier, and B. Lascoup, "Time Delay Estimation for Acoustic Source Location by Means of Short-Time Cross-Correlation", *IEEE International Conference on Sensors*, Limerick, Ireland, october 2011.

[2] B. Woodacre, "TDOA Positioning and TOA-based Calibration for Precision Location", Master's thesis, *Worcester Polytechnic Institute*, (2004).

[3] T. Ajdler, I. Kozintsev, R. Lienhart, M. Vetterli, "Acoustic Source Localization in Distributed Sensor Networks", *Asilomar Conference on Signals, Systems and Computers*, Pacific Grove, CA, **2**, 1328-1332, (2004).

[4] M.L. Fowler and Xi Hu, "Signal Models for TDOA/FDOA Estimation", *IEEE Transactions on Aerospace and Electronic Systems*, **44**, 1543-1550, (2008).

[5] S.M. Kay, "Modern Spectral Estimation - Theory & Application", *Prentice-Hall*, (1988).

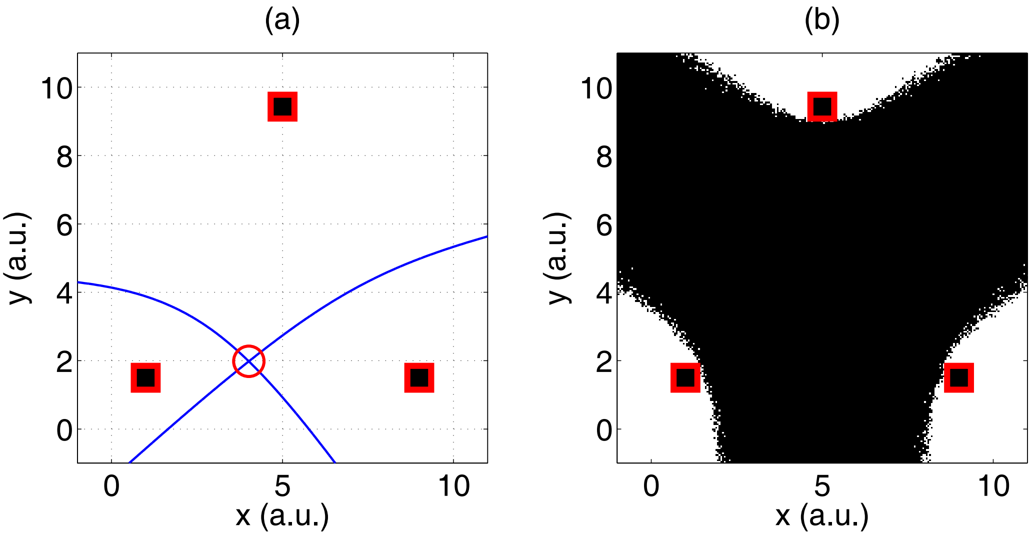

Figure 1: Location of the 3 sensors (ref. sensor at the top of the plate) (a) - Valid zone of measurement (black) (b).

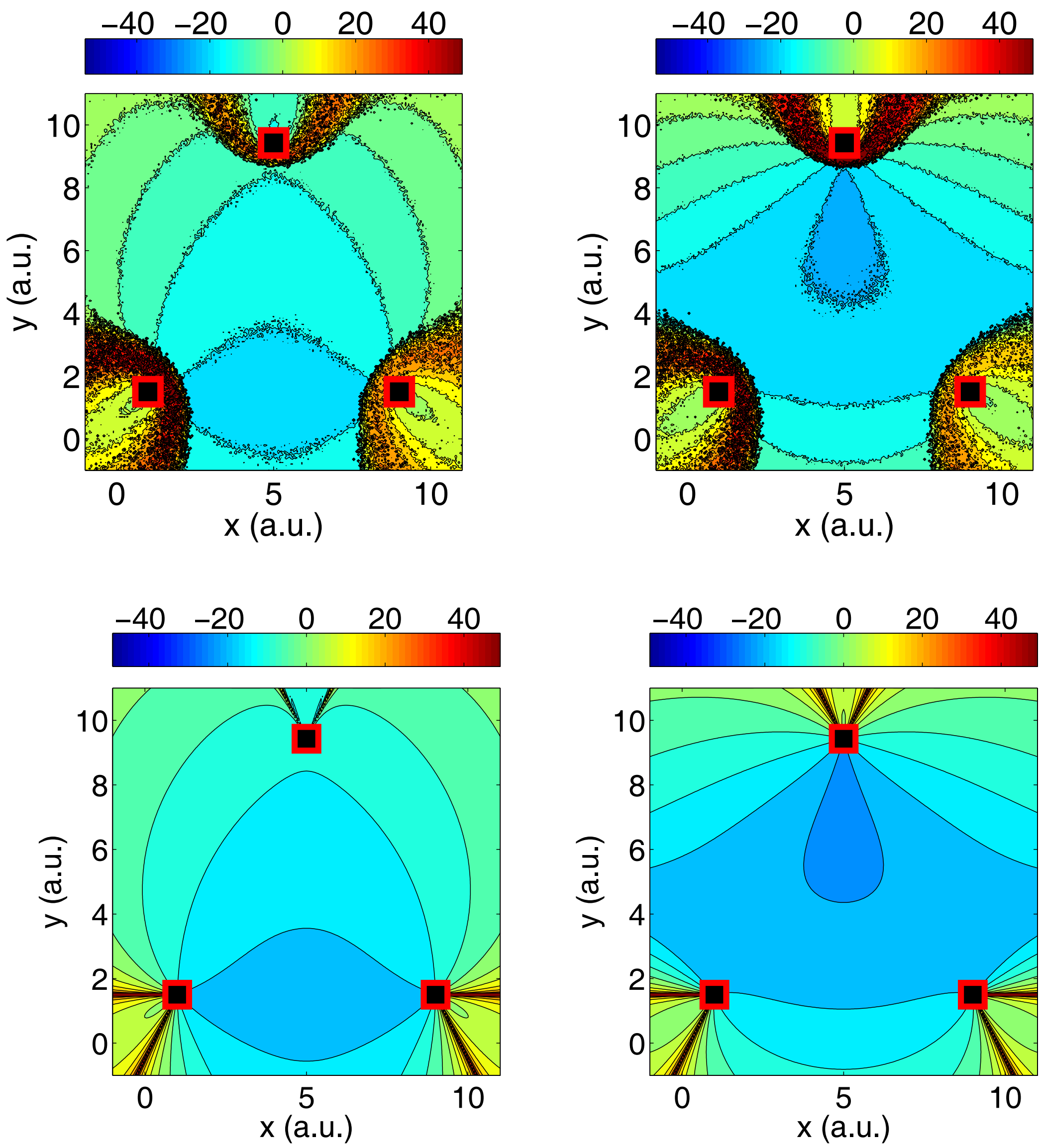

Figure 2: var(x) (upper left) - var(y) (upper right) - CRB(x) (down left) - CRB(y) (down right) .

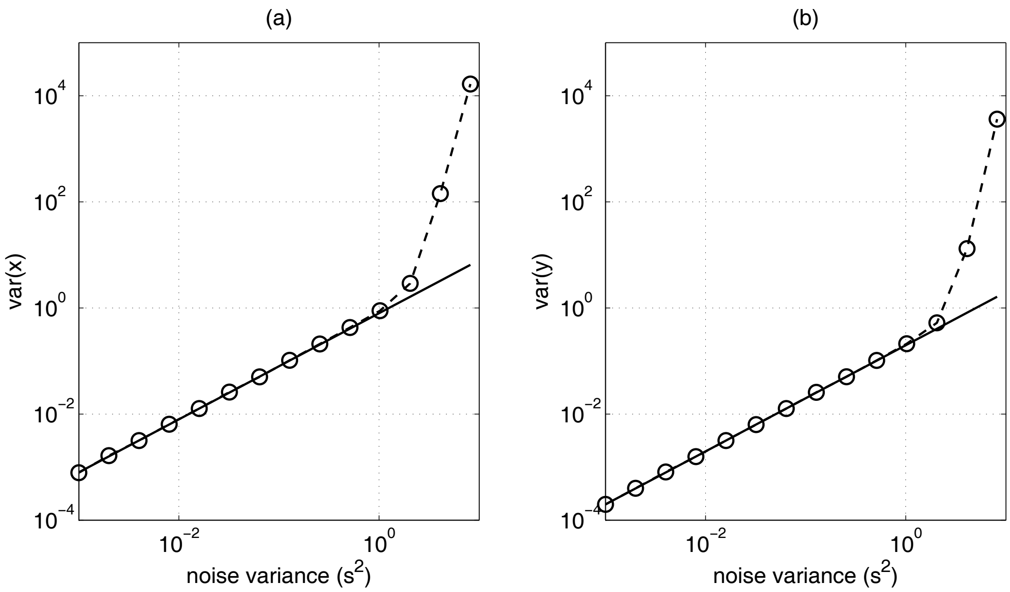

Figure 3: CRB(x) (a) and CRB(y) (b) versus variance of noise for the coordinate pair $(x, y) = (4.5, 4.5)$.